Analysis and optimization of the threshing and clearing system of edible bean harvesting equipment

Xinzhou Zhang[1, *], Zhiyuan Zheng[1], Shixun Fu[1] and Xianfei Xia[2]

[1] School of Mechanical Engineering, Jiangsu University, Zhenjiang, Jiangsu 212013, China

[2] Nanjing Institute of Agricultural Mechanization, Ministry of Agriculture and Rural Affairs, Nanjing, Jiangsu 210014, China.

Corresponding author: zhangxinzhou1984@126.com

Abstract

Currently, the mechanization level of edible bean harvesting in China is relatively low, and corresponding production equipment is in shortage, especially during the harvesting stage, where most processes require manual cutting, threshing, and cleaning. This results in low work efficiency and high production costs, which significantly hinders the development of the industry. Therefore, research on suitable threshing and cleaning equipment for edible beans is of utmost importance for the growth of the edible bean industry. Based on literature and existing equipment, this article analyzes and optimizes the vertical axial flow threshing device among various threshing device types. With an understanding of the working principle and threshing process of the vertical axial flow threshing device, this article optimizes and analyzes a new type of vertical axial flow threshing device to achieve the goal of low-breakage and high-cleaning threshing for edible beans. By utilizing the UG finite element analysis module, a static analysis is performed on the front-closed and rear-open combined threshing device, and based on a comprehensive analysis of the results, the optimized structural parameters of the threshing device's grooved bar block are designed.

Keywords

Edible beans, Threshing device, Threshing elements, Finite element analysis.

1. Introduction

Edible beans refer to the general name of leguminous crops that are mainly harvested for their seeds and are consumed by humans, excluding soybeans. They include broad beans, kidney beans, peas, mung beans, adzuki beans, etc. China has a cultivation area of about 100 million mu (about 6.67 million hectares) of edible beans annually, with the total output accounting for 60% of the global total [1-2]. Both the cultivation area and variety rank first in the world. Most edible beans have irregular seed shapes and great differences in geometric dimensions. In particular, during the mechanical harvesting process of heterogeneous seeds like broad beans and kidney beans, as well as those with high water content, seed damage and loss are extremely high. The comprehensive loss rate (crushing, cutting platform and inclusion loss) of some models is higher than 30%. For example, the maximum length-to-width ratio of kidney beans and cowpeas can reach 5, and the flat-to-flat ratio of broad beans is greater than 3. Meanwhile, most edible bean varieties are indeterminate inflorescences. To ensure high yield and reduce harvesting losses, harvesting needs to be done before some seeds reach full maturity. Taking mung beans as an example, about 10% of the pods are not fully mature during mechanized one-time harvesting, and the water content of the material is relatively high at this time.

Edible beans are mostly produced in medium and small-scale farms, and most existing small and medium-sized grain combine harvesters employ the methods of open pin tooth single-longitudinal axis threshing, wind-sieve cleaning, and auger material conveying. Specifically, the open pin tooth threshing mechanism often results in a high threshing breakage rate and dirty surfaces of edible bean grains during threshing. Since edible bean plants contain a high level of water, using traditional combine harvesters tends to lead to the blocking of cleaning sieve holes and malfunctioning of the machine. Therefore, the development of a combine harvester suitable for edible bean harvesting can significantly reduce grain breakage and carryover loss.

The all-new New Holland CSX7000 series combine harvester selects multiple tangential threshing drums as its threshing device, and the cooperation between these threshing drums greatly improves the performance and threshing efficiency of the threshing device [1]. The TUANCO 400-300 combine harvester developed in Germany adopts the APS threshing system, where the threshing elements of the threshing drum are traditional helical bars. The Axial-Flow series combine harvester developed in the United States is equipped with the AFX threshing drum, which uses short helical bars as threshing elements in the middle section. This design interacts more gently with edible bean plants, resulting in a low grain breakage rate. The LEXION760 series combine harvester developed in Germany can significantly improve grain threshing efficiency and reduce machine power consumption.

Peng Yuxing and his team from Hunan Agricultural University have developed a single longitudinal threshing drum to address the issue of threshing drum blockage caused by excessive crop feeding [3]. Li Yaoming and his team from Jiangsu University have designed a short-helix-bar-and-plate-tooth threshing drum [4-5]. Compared to the pin-tooth threshing drum, this threshing drum consumes less power when threshing rice and produces less impurity content in the threshing mixture [6-7]. Wang Zhendong and his team from China Agricultural University have designed a helical-bar threshing element, which significantly reduces grain breakage rates [8].

As a miscellaneous grain crop, edible beans have not received sufficient attention, and the research and development of specialized production machinery for them is even rarer. Most bean varieties have irregular grain shapes and significant differences in geometric sizes, especially for beans with irregular grain shapes like broad beans and kidney beans, as well as beans with high water content. During the mechanical harvesting process, grain damage and loss are particularly high, with the comprehensive loss rate (including breakage, cutting table, and carryover loss) of some models exceeding 30%.

Based on the existing combined threshing device, this paper proposes an optimized front-closed and rear-open combined threshing device. By segmenting and combining closed and open drums, the goal of low-damage and high-cleanliness threshing of edible beans is achieved. This optimized design aims to address the challenges posed by the irregular grain shapes and high water content of edible beans, reducing grain damage and loss during the harvesting process.

2. The design of a combined threshing device with a closed front and an open rear structure

2.1. Working Principle Analysis

In the realm of grain crop production, mechanization in edible bean production remains a weak link, and mechanized harvesting, in particular, stands as "the weakest link among the weak." This article provides an analysis of the design and working principles of a new threshing device, namely, the combined threshing device with a closed front and an open rear structure.

As shown in the figure, the three-dimensional structure of the combined threshing device with a closed front and an open rear comprises a closed threshing cylinder and an open threshing structure that work in coordination. The front end of the threshing device is equipped with a

ISSN: 1813-4890

feeding auger and a guide cone, allowing the edible bean plants to smoothly enter the threshing cylinder. The middle section consists of a short closed cylinder with a small diameter, and the threshing elements on the closed cylinder are long and short grooved bars arranged according to different needs. The rear end features an open threshing structure, with threshing elements composed of long grooved bars and bar teeth. At the end of the device, the threshing impurities can be discharged out of the machine. Beneath the closed cylinder and the open threshing structure is a concave plate screen with adjustable threshing gaps. The speed of the threshing cylinder is adjustable, and the gaps between the nail teeth/grooved bars and the concave plate screen are also adjustable.

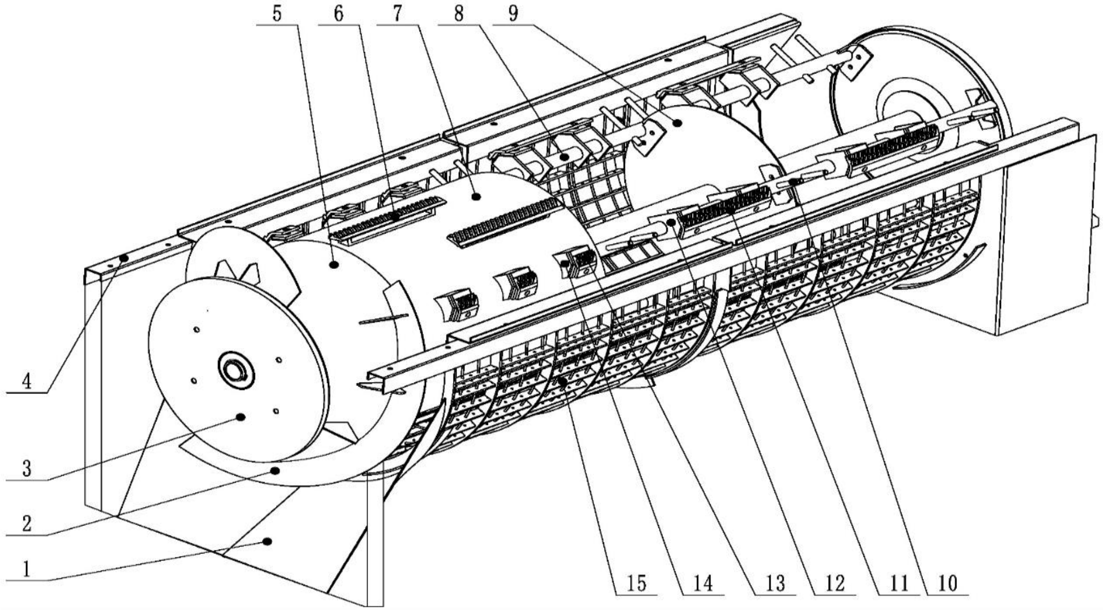

Figure 1: 3D Structural Diagram of the Combined Front-Closed and Rear-Open Threshing Device

The components of the threshing device are: 1-Feed guide plate, 2-Feeding auger, 3-Adjustable mounting base for threshing cylinder, 4-Machine frame, 5-Guide cone, 6-Long grooved bars for closed threshing, 7-Front section of the closed threshing cylinder, 8-Threshing crossbar, 9-Crossbar fixing plate, 10-Threshing nail teeth, 11-Long grooved bars for open threshing, 12-Adjustable mounting base for grooved bars, 13-Short grooved bars for closed threshing, 14-Adjustable mounting base for short grooved bars, 15-Concave plate screen assembly. The combined threshing cylinder with a closed front and an open rear design features a closed cylinder at the front and an open threshing structure at the rear. The threshing elements on the closed cylinder are a combination of long and short grooved bars. The open structure at the rear consists of a combination of grooved bars and nail teeth, which can achieve continued threshing and separation of incompletely threshed grains, as well as separating the grains from threshing impurities.

The working principle of this threshing device is as follows: The threshing cylinder mounting base 3 is installed onto the combine harvester frame, allowing for adjustments to the corresponding gaps and positions through the system. The threshing material is conveyed by the spiral feeding action of the feeding auger 2 from the feed guide plate 1 through the guide cone into the interior of the threshing cylinder. The threshing cylinder consists of a closed cylinder 7 and a rear open structure. The front closed cylinder is arranged with threshing elements, including long grooved bars 7 and short grooved bars 13, installed on the adjustable mounting bases 14. These bases allow for the adjustment of the distance between the grooved bars and the cylinder. The rear open threshing structure consists of threshing crossbars 8, crossbar fixing bars 9, threshing nail teeth 10, adjustable mounting bases 12 for grooved bars, and long grooved bars 11 for open threshing. The distance between the nail teeth and long grooved bars is also adjustable. After the threshing material is rubbed and struck by the closed and open threshing cylinders, the grains fall through the gaps formed by the concave plate screen assembly 15 to the lower end, while the threshing impurities are discharged from the end of the threshing cylinder.

The combined threshing cylinder with a closed front and an open rear design features a closed cylinder at the front and an open threshing structure at the rear. The threshing elements on the closed cylinder are a combination of long and short grooved bars. Through the rubbing action of this combined structure, the grooved bars effectively separate the grains from the pods, minimizing the damage to the grains by the threshing elements at the rear. This helps reduce impact losses and breakage. The open structure at the rear, consisting of a combination of grooved bars and nail teeth, enables the continued threshing and separation of incompletely threshed grains, effectively separating the grains from threshing impurities. This comprehensive design reduces the threshing breakage rate and improves the threshing separation efficiency.

2.2. Design Analysis of the Threshing Elements Structure

Types of threshing elements include grooved bars, nail teeth, bow teeth, and impellers. According to the JB/T9778.2-1999 standard, "Type, Size, and Technical Requirements of Grooved Bar Threshing Cylinders," grooved bar threshing elements are classified into Type A and Type D. Type D grooved bars are preferred (as shown in Figure 2), with a thickness of a and d set at 6mm, the length of the effective curved surface at the top, c, at 26mm, and the length b at 24mm.

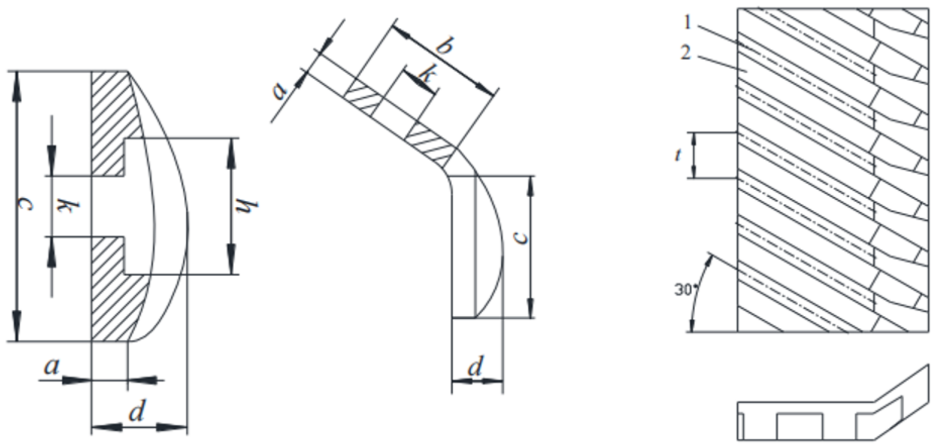

(a) Type A (b) Type D (c) Grooved Bar Design Diagram

Figure 2: Grooved Bar Type and Design Diagram

As shown in Figure 3, the grooved bar has concave pits and convex ridges on its top surface, which enhance its grip on edible bean plants and intensify the friction and collision between the grooved bar and the plants. The front inclined surface of the grooved bar has through holes that allow it to be bolted to the grooved bar holder, making installation and removal more convenient. Based on literature analysis [9-10], we know some geometric parameters of edible bean pods. The pod of the broad bean is cylindrical, with a length of 5-10 cm and a width of 2-3 cm. The pod of the green bean is also cylindrical, with a length of 10-15 cm and a width of approximately 1 cm. The pod of the pea is ellipsoid-shaped, with a length of 2.5-10 cm and a width of 0.7-1.4 cm. In the design diagram of Figure 2, the concave pit width is 8 mm, and the convex ridge width is 5 mm, thus the value of t in Figure 2 is 13 mm.

Figure 3: 3D Model of Grooved Bar

In the threshing device, the rod teeth are welded onto the threshing rods of the rear open-type threshing structure according to the hole positions. As analyzed in the previous section on the threshing process, the rear open-type threshing structure serves the purpose of secondary threshing and separating the grain from the straw. Compared to grooved bars, rod teeth exert a greater force on the crop, effectively threshing stubborn grains and agitating and breaking the straw. The rod teeth are closely related to the fragmentation size of the threshing impurities. If the fragmentation size is too large, it can lead to blockage of the concave sieve holes, thereby reducing the discharge speed of threshing impurities and the speed of grains entering the cleaning system, resulting in an increased loss rate of grain entrainment. Conversely, if the fragmentation size is too small, such as smaller than the size of the concave sieve holes, more impurities will enter the cleaning system, leading to increased load on the cleaning system and higher energy consumption. Therefore, it is crucial to strictly determine the structural dimensions of the rod teeth. According to the analysis in the "Agricultural Machinery Design Manual," a rod tooth height of 123mm, a diameter of 12mm, and a chamfered design at the top of the rod teeth are selected. This chamfered design can mitigate the impact force of the rod teeth on the grains, reducing grain breakage.

3. Optimization of Grooved Bar Blocks for Threshing Elements

3.1. Structure of the grooved bar block

As shown in Figure 4, the structure of the grooved bar block mainly includes geometric parameters of the top curved surface and the angle of the front inclined surface θ. The geometric parameters of the top curved surface consist of the width of the convex ridge W, the height of the high point of the top convex ridge h, the angle of inclination of the convex ridge β, and the shape of the top curved surface [8]. When the grooved bar block comes into contact with the edible bean plants, the front inclined surface pushes the plants to the top curved surface, making the collision between the grooved bar block and the plants more gentle. The cooperation between the convex ridge of the grooved bar block, the top cover of the threshing device, and the concave sieve exerts a certain amount of pressure on the edible bean plants, facilitating the threshing process through rolling and rubbing. Each structural parameter of the grooved bar block has a different effect on the threshing of the edible bean plants. For instance, the shape of the convex ridge on the top of the grooved bar block affects the intensity of rolling and rubbing. The different widths of the convex ridge and the concave pit result in different contact areas with the edible bean plants, thereby affecting the pressure exerted on the plants within the threshing device. Additionally, the angle of inclination of the convex ridge influences the direction of the edible bean plants.

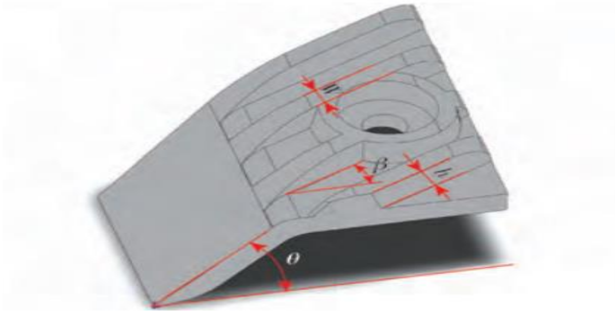

Figure 4: Schematic Diagram of the Grooved Bar Block Structure

3.2. Finite Element Model

Using the NX Nastran module in the UG software for finite element analysis, this solver allows for nearly unlimited degrees of freedom for the analysis object, achieving high accuracy in various aspects of the solution. Below is the process of finite element analysis for the grooved bar block [11]:

(1) To establish a 3D assembly model of the threshing device with a closed front and open rear structure (as shown in Figure 5), create 3D models for each component of the threshing device. Afterward, import all the components into an assembly environment and perform assembly and constraints based on their respective positional relationships.

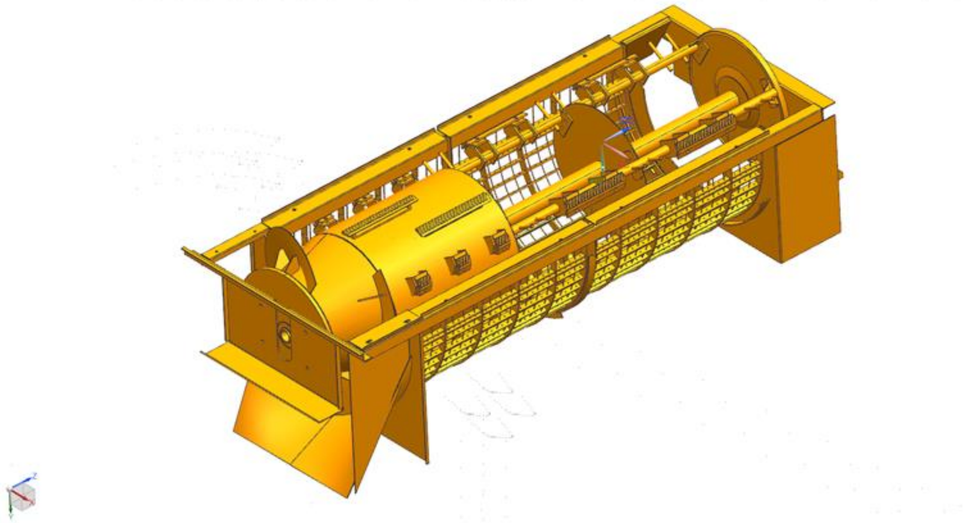

Figure 5: 3D model of the threshing device

(2) Establishing a finite element analysis model involves optimizing the grooved bars and grooved bar holders on the closed cylinder. To improve computational efficiency, the threshing device model is simplified by removing some components, resulting in an assembly model primarily composed of closed short grooved bars and grooved bar holders, as shown in Figure 6.

Entering the pre- and post-processing modules in UG, materials and mesh division are assigned to the two components in the simplified model of the grooved bar block. During this process, geometric features that have minimal impact on the analysis results, such as rounded corners, chamfers, and threaded holes, can be eliminated or suppressed in the idealized component model. Both the grooved bar and the grooved bar holder are not sheet bodies or shells, therefore, 3D meshing is chosen for division. The tetrahedral element is used for mesh analysis of the 3D model, as it provides flexibility in approximating complex geometric shapes.

The number of meshes divided will have an impact on the scale and accuracy of the calculation. In general, when the number of meshes is higher, the calculation accuracy increases but the calculation scale and time increase accordingly. Conversely, with a lower number of meshes, the calculation accuracy decreases while the scale and time are reduced. Therefore, the determination of the mesh number should consider both calculation accuracy and scale. To ensure the accuracy of the results, the mesh division unit size for the simplified grooved bar block is set to half of the automatic unit size. The grooved bar block model after mesh division is shown in Figure 7.

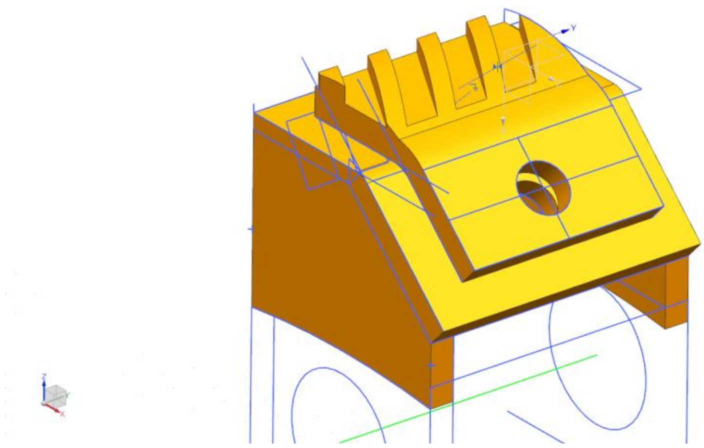
Figure 6: Simplified model of the grooved bar block

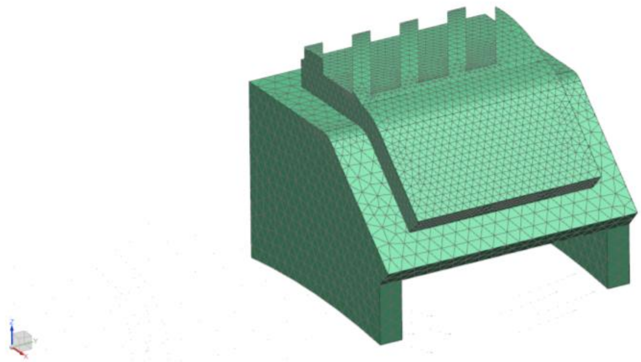
Figure 7: Grooved bar block mesh division model

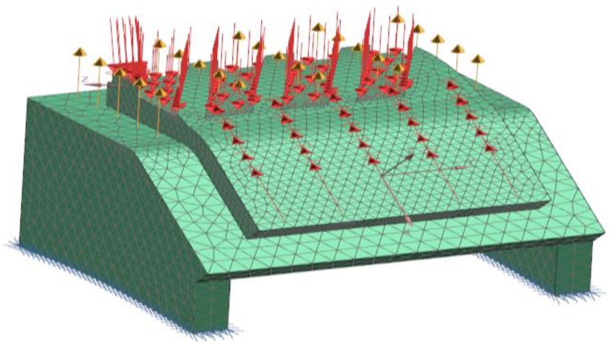
Figure 8: Constraints and Loads

(3) Applying Constraints and Loads. After establishing the finite element analysis model of the grooved bar block, we proceed to the simulation environment. In the threshing process of edible bean plants, the grooved bar block is welded onto the threshing cylinder, so a fixed constraint is applied to the grooved bar block. During operation, the grooved bar block will be subject to forces from multiple directions, resulting in a complex stress condition. Its static and dynamic characteristics depend on various factors. To facilitate the deformation analysis of the model, some simplifications are made to the actual working conditions of the grooved bar block. Assuming that the protruding ridge at the top of the grooved bar block mainly bears a normal

ISSN: 1813-4890

pressure and tangential force of 16.5 MPa, the concave area bears a normal force of 12.8 MPa, and the front inclined surface bears a tangential force of 5.12 MPa. The loads are applied to the finite element analysis model of the threshing device [13], as shown in Figure 8.

3.3. Finite Element Analysis Results

By analyzing the finite element model of the grooved bar block, the analysis results are shown in Figures 9 and 10. From the elastic deformation displacement diagram of the grooved bar block, it can be observed that due to the main normal pressure acting on the protruding ridge and concave surface of the grooved bar, the upper surface of the grooved bar holder experiences a downward concave deformation, and the rounded corner transition of the grooved bar undergoes a bending deformation. The maximum deformation displacement is 0.058 mm, while the minimum deformation displacement is 0 mm (under ideal conditions). From the stress analysis diagram of the grooved bar block, it is evident that the left and right side surfaces of the grooved bar holder and the upper surface of the rounded corner transition of the grooved bar are subjected to relatively large tensile stress, with a maximum tensile stress of 37 MPa. The upper surface of the grooved bar holder experiences a relatively large compressive stress, with a maximum compressive stress of 192.78 MPa.

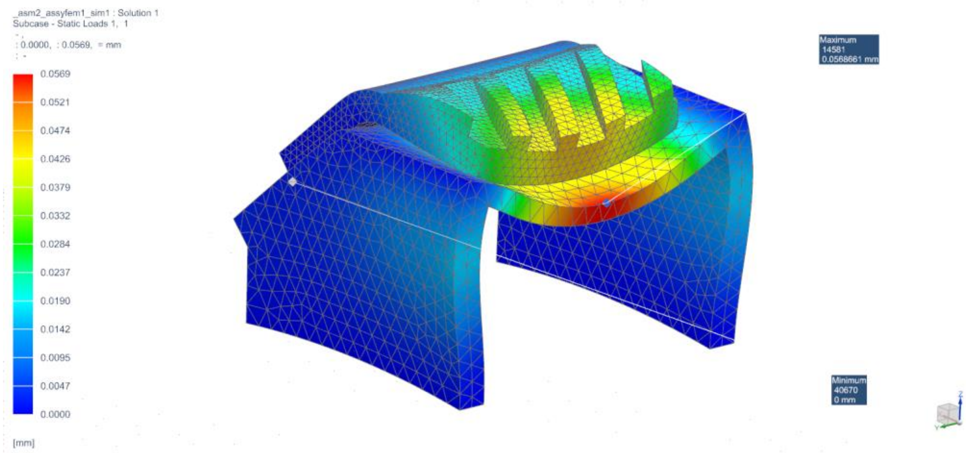

Figure 9: Deformation displacement contour plot of the grooved bar block

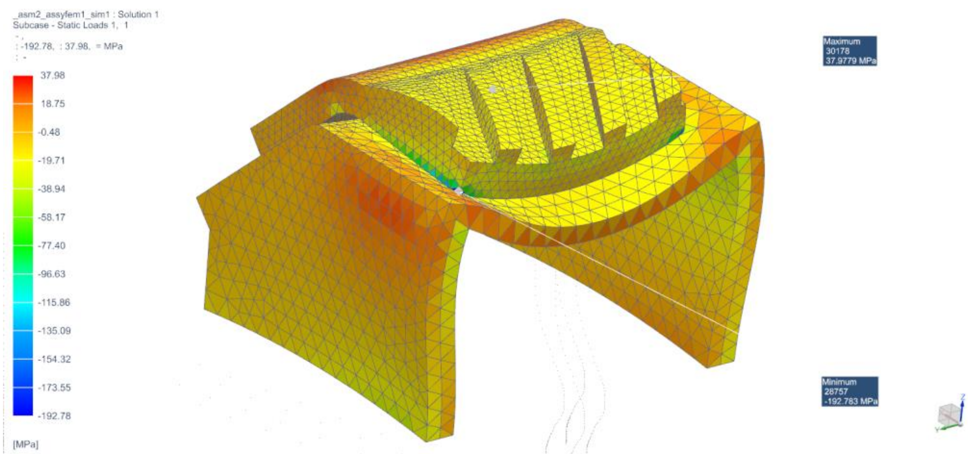

Figure 10: Stress contour plot of the grooved bar block

3.4. Optimization of the Grooved Bar Block

Due to the main normal pressure acting on the protruding ridge and concave surface of the grooved bar, the upper surface of the grooved bar holder experiences a downward concave deformation, and the rounded corner transition of the grooved bar undergoes a bending deformation. The maximum deformation displacement is 0.058 mm, while the minimum deformation displacement is 0 mm (under ideal conditions). From the stress analysis diagram of the grooved bar block, it can be seen that the left and right side surfaces of the grooved bar holder and the rounded corner transition of the grooved bar are subjected to relatively large tensile stress, with a maximum tensile stress of 37 MPa. The upper surface of the grooved bar holder is under relatively high compressive stress, with a maximum compressive stress of 192.78 MPa. By conducting finite element analysis with different materials assigned to the grooved bar block and modifying its structure, an optimal optimization scheme for the grooved bar block can be obtained.

Modification of the geometric shape of the grooved bar block: According to market research and literature review, the pod length of broad bean ranges from 5 to 10 cm, with a width of 2 to 3 cm; the pod length of kidney bean ranges from 10 to 15 cm, with a width of approximately 1 cm; and the pod of garden pea is ellipsoid-shaped, ranging from 2.5 to 10 cm in length and 0.7 to 14 cm in width. Analysis indicates that the contact stress between the edible bean kernels and the concave part of the grooved bar is smaller than that of the convex ridge part. To ensure sufficient contact between the concave part and the edible bean kernels, the width of the concave part is set at 20 mm, and the width of the convex ridge is 15 mm. The long-shaped grooved bar not only rubs the edible bean plants but also causes high-frequency vibrations in the radial direction of the threshing cylinder, which facilitates threshing and separation of the edible bean kernels. Therefore, all grooved bars are changed to long grooved bars with a length of 180 mm, while other structural parameters remain unchanged. Based on the stress diagram analysis of the grooved bar block mentioned earlier, the deformation of the grooved bar holder mainly occurs on the upper surface and left and right sides. Therefore, the thickness of the upper surface and sides of the grooved bar holder is increased by 2 mm to reduce stress. The spacing between two grooved bar holders is 90 mm. The optimized grooved bar block is shown in Figure 11.

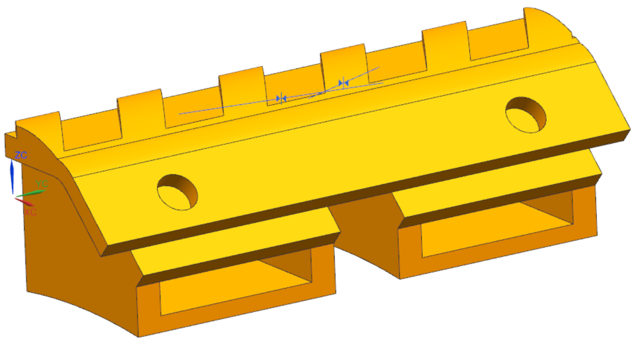

Figure 11: The optimized grooved bar block

A finite element model was established for the optimized grooved bar block, and the resulting deformation displacement diagram and stress diagram are shown in Figures 12 and 13. As can be seen from the deformation displacement diagram of the grooved bar block, compared with the unoptimized version, the maximum deformation displacement has decreased by approximately one-fifth, with a value of 0.043 mm. The maximum deformation occurs on the upper surface of the grooved bar holder. According to the stress diagram, the maximum tensile stress on the grooved bar block is 40.3 MPa, located in the concave part of the grooved bar. The maximum compressive stress on the grooved bar block is 106 MPa, located on the lower surface of the rounded corner transition of the grooved bar. Compared with the unoptimized grooved bar block, the tensile stress remains largely unchanged, while the compressive stress has significantly decreased.

ISSN: 1813-4890

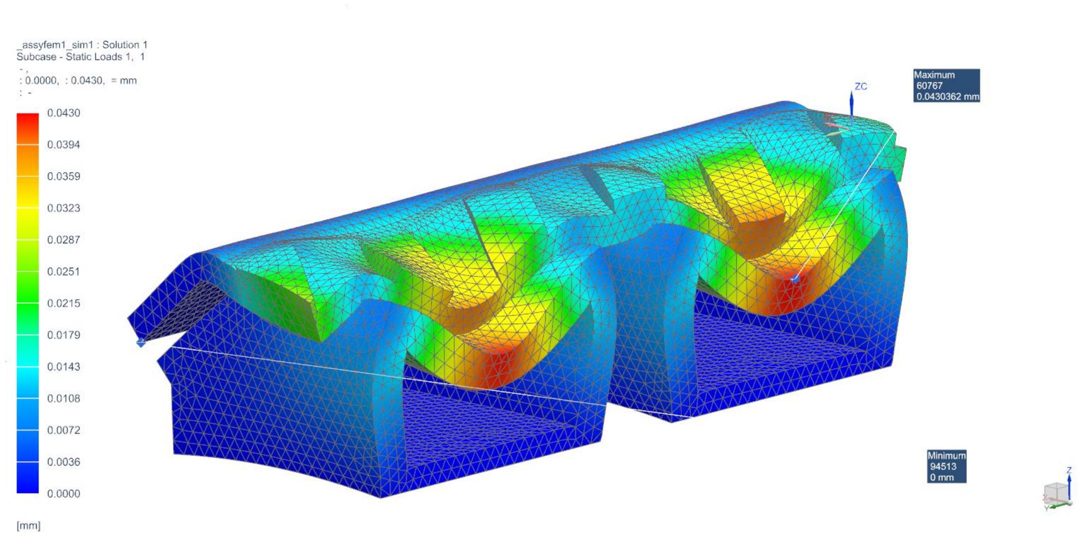

Figure 12: Deformation displacement contour plot of the optimized grooved bar block

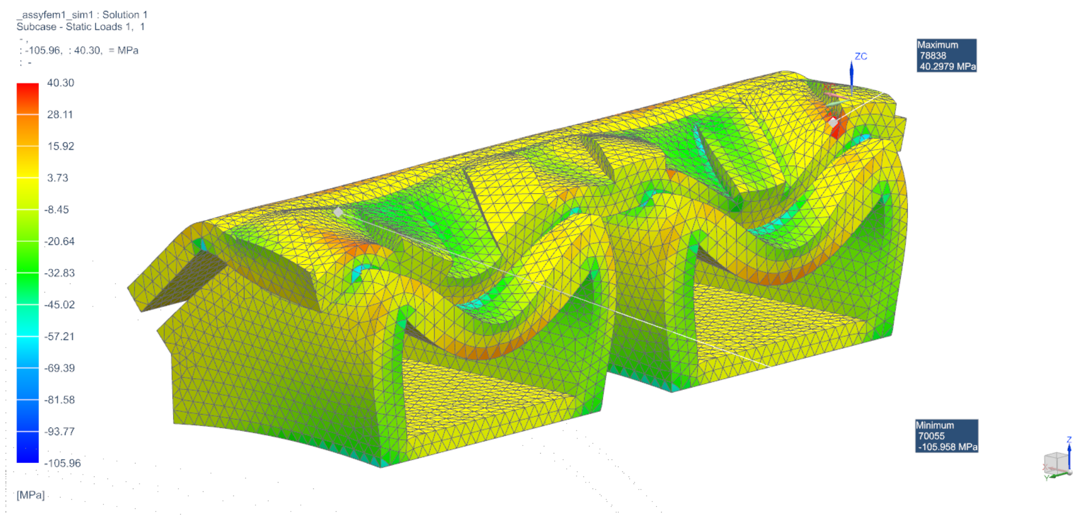

Figure 13: Stress contour plot of the optimized grooved bar block

4. Conclusion

This article analyzes the threshing principles and processes of a new type of longitudinal axial flow threshing device, specifically the front-closed and rear-open combined threshing device. It also conducts analysis and optimization of the device's components to determine a threshing device that meets the operational, economic, and safety requirements. The main research conclusions of this article are as follows:

(1) The article discusses the existing edible bean threshing devices both domestically and internationally, summarizing the advantages and disadvantages of different types of threshing devices. Based on the new front-closed and rear-open combined threshing device, it analyzes the threshing principles and processes of the threshing device, determining the geometric parameters of the main components within the threshing device.

(2) A finite element model of the original grooved bar block was established, and a comparative CAE analysis was conducted based on its actual working conditions. This ultimately led to the determination of the optimized structure, material, and layout of the grooved bar block. To ensure sufficient contact between the edible bean plants and the grooved bars, the optimized grooved bar ridge width is 15mm, the pit width is 20mm, and the length of the grooved bar block is 180mm, while other structural parameters remain unchanged.

Acknowledgements

This research was funded by the Jiangsu Province Agricultural Science and Technology Innovation Fund Project (No. CX(21)3145).

References

[1] Xia Xianfei, Chen Qiaomin, Xiao Hongru, et al. Research on current status and developing strategy of pulses crops mechanized harvesting technology in China [J]. Journal of Chinesce Agricultural Mechanization, 2019,40(05):22-28. (In Chinese)

[2] Zhan Caixue, Chen Qiaomin, Xiao Hongru, et al. Applicability analyses of combined harvest threshing and cleaning device for edible beans [J]. Journal of Chinese Agricultural Mechanization, 2020, 41(6): 13-19. (In Chinese)

[3] Peng Yuxing, Li Xu, Liu Dawei, et al. Design and performance experiment of a threshing cylinder with longitudinal single axial flow [J]. Journal of Hunan Agricultural University (Natural Sciences), 2016, 42(5):554-560. (In Chinese)

[4] Li Yaoming, Tang Zhong, Xu Lizhang, et al. Power Analysis and Experiment on Longitudinal Axial-threshing Unit Test-bed [J]. Transactions of the Chinese Society for Agricultural Machinery, 2011, 42(6): 116-120. (In Chinese)

[5] Xu Lizhang, Li Yaoming, Wang Chenghong, et al. A Combinational Threshing and Separating Unit of Combine Harvester with a Transverse Tangential Cylinder and an Axial Rotor [J]. Transactions of the Chinese Society for Agricultural Machinery, 2014, 45(2): 105-108, 135. (In Chinese)

[6] Li Yaoming, Li Hongchang, Xu Lizhang. Comparative experiments on threshing performance between short-rasp-bar tooth cylinder and spike tooth cylinder [J]. Transactions of the CSAE, 2008, 24(3): 139-142. (in Chinese)

[7] Li Yaoming, Li Hongchang, Xu Lizhang, et al. Performance Test of Short-rasp-bar of Axial Flow Threshing and Separating Unit [J]. Transactions of the Chinese Society for Agricultural Machinery, 2009, 40(7): 88-92. (in Chinese)

[8] Wang Zhendong, Cui Tao, Zhang Dongxing, et al. Design and Experiment of Rasp Bar Threshing Element of Corn Combine Harvester [J]. Transactions of the Chinese Society for Agricultural Machinery, 2021, 52(9): 115-122. (in Chinese)

[9] Wang Qinxia, Wang Chi, Lin Yi. Comparative test of new varieties of broad bean [J]. Modern Agricultural Science and Technology, 2022(7): 37-42. (in Chinese)

[10] Chen Min, Feng Huangshu, Wang Huike, et al. Comparative Test of Snap Bean Varieties in Luodian County [J]. Agricultural Technology Service, 2022, 39(2): 23-24. (in Chinese)

[11] Zhang Jian, Gan Luping, Guan Wanwu. Design and finite element analysis of buckwheat threshing device [J]. Journal of Chinese Agricultural Mechanization, 2019, 40(7): 7-12. (in Chinese)

[12] Hu Aimin, Long Ming. UG NX 12 Chinese Edition Self-study Manual for Dynamics and Finite Element Analysis [M]. Beijing, Posts & Telecom Press, 2019. (in Chinese)

[13] Dun Guoqiang, Chen Haitao, Liu Huanyu, et al. Soybean Impacting Simulation Analysis in Threshing Process Based on SolidWorks Simulation and Orthogonal Test [J]. Journal of Graphics, 2015, 35(5): 724-729. (in Chinese)